Evaluation of single-phase and two-phase propane release via CFD simulation applied to the hazardous area classification

Natalya A. B. de Almeida[1], Claudemi A. Nascimento[1], José J. N. Alves[1]

[1]*Dept. of Chemical Engineering, Federal University of Campina Grande*
882 Aprígio Veloso, 58429-900, Paraíba/Campina Grande, Brazil
natalya.amelia@eq.ufcg.edu.br, claudemi.alves@eq.ufcg.edu.br, jailson@eq.ufcg.edu.br

Abstract. Different leakage scenarios can occur in industries that handle flammable substances. Fugitive releases are frequent leakage scenarios that can result in explosive atmosphere formation. These releases can be single-phase or two-phase, depending on the storage conditions. For two-phase releases, the leakage condition needs to consider the thermodynamic state in the storage and the orifice. In this context, methods for hazardous area classification must be used to ensure process safety. One of the methods used for area classification and recommended by the international standard IEC 60079-10-1(2015) is Computational Fluid Dynamics (CFD), a numerical tool that accurately assesses many different release scenarios. Therefore, this work aims to contrast different approaches from CFD simulations for liquefied propane release scenarios in an open and unobstructed environment. A pseudo-source approach was assumed to simulate the post-expansion region for both conditions of thermodynamic equilibrium and superheated liquid in the release orifice. The same pseudo source approach was considered in the case where only gas is released. The Eulerian-Lagrangian approach was applied to the multiphase simulation, and the Eulerian approach for the gas phase simulations in both single and two-phase simulations. The liquid and gas temperature results showed the behavior of an expected flash release when dealing with liquefied gas depressurization. The extent and gas cloud volume results delimited by specific concentrations were quite similar for both scenarios. The pseudo-source approach considering only the gas required a shorter simulation time without losing the accuracy of the results compared to the two-phase simulations. It indicated a significant gain on reducing the simulation effort required for hazardous area classification assessment in two-phase releases scenarios when there is no pool formation.

Keywords: two-phase release, CFD simulation, hazardous area classification.

1 Introduction

In industry, the storage conditions for flammable substances are defined according to desired physical state to be stored. Whether this material is stored or transported in the process, the equipment involved becomes a possible sources of release of these substances into the atmosphere. In this context, two different release scenarios can occur. The release can be all liquid or gaseous (single-phase flow) or both states (two-phase flow). Both scenarios are related to parameters that define them. Some of the main parameters are the substance and its physicochemical properties, the initial condition of the process (storage condition), the duration of release, the characteristics of the hole, and the atmospheric conditions of the environment whither release the material [1, 2].

Through the knowledge of release scenarios and to ensure process safety, the hazardous area classification method emerges to identify areas where the atmosphere of flammable gas may occur. The international standard IEC 60079-10-1 (2020) [4] provides guidelines for the application of this method and recommends the use of Computational Fluid Dynamics (CFD) to simulate release scenarios where the interaction of multiple factors occurs, such as the presence of obstacles and position concerning the ground. A classified area classification has as main results the type of zone and the extent of the classified area.

Different approaches can be made in CFD considering the two-phase flow release scenarios and the needing

to obtain information for area classification. This work considered two of these approaches, one from the two-phase region and the other from the single-phase region. In the latter case, it starts from the point where the liquid completely evaporates. For both approaches, pseudo-source treatment was used, in addition to having homogeneous equilibrium conditions (saturation condition) and non-equilibrium conditions (superheated liquid condition) in the release orifice. The evaluation of extent and volume results for area classification purposes by CFD simulations is made. Thus, this work aims to simulate and compare different approaches in CFD from a scenario of the release of liquefied propane, stored under pressure (liquid / saturated steam), to an open and unobstructed environment. This work does not deal with pool formation scenarios.

2 Hazardous area classification

Hazardous area classification corresponds to a method that aims to classify an area likely to have an explosive atmosphere. From the area classification, it becomes possible to select, install and operate the equipment properly, ensuring process safety [4]. The existence of regulatory standards for the hazardous area classification provides guidelines for their execution.

The international standard IEC 60079-10-1 addresses the area classification of flammable gas atmospheres, characterizing the type and extent of the zone. Zones are defined according to the frequency of occurrence and duration of the explosive atmosphere; the zone extent represents the distance from the source of release to where the dilution of gas concentration by air reached a concentration of interest, which can be LFL (Lower Flammability Limit), ½ LFL or ¼ LFL.

3 Scenarios of a two-phase release

As described by Calay and Holdo (2008) [5], the flow rate of discharge and its phase is dependent on the release scenario. When evaluating the pressurized liquefied gas storage scenarios, two possible storage conditions may occur. The gas storage conditions can be saturated, so two-phase inside the reservoir and in physical equilibrium in the release orifice. Likewise, the gas can be stored as a subcooled liquid, concerning the saturation temperature at the storage pressure, however be superheated concerning the ambient conditions. Depending on the orifice diameter and the ratio of tube length (can be represented by tank wall thickness), the flow may become two-phase, and, therefore, present in thermodynamic equilibrium at the release orifice. Otherwise, the flow may be in a non-equilibrium condition, presenting itself as a superheated liquid in the release orifice [3,6].

To obtain the characteristic data of a two-phase release, it's necessary to know the information from the storage and the release orifice, so it will be possible to obtain the parameters in the post-expansion region. Initially, the storage parameter needs to be determined. It could be the temperature (T_s) or pressure (P_s), under saturation conditions, calculated by the Antoine equation:

$$\log_{10} P_s = A - \frac{B}{T_s + C} \tag{1}$$

Observing the equilibrium and non-equilibrium conditions in the mentioned release orifice, it follows the determination of the parameters for each one of the conditions in the orifice.

In the first case, where the two-phase flow in thermodynamic equilibrium is present in the orifice, the pressure inside the reservoir will be greater than the pressure in the orifice (P_o) and this can be represented by [6]:

$$P_o = 0.85 P_s \tag{2}$$

Based on the estimate of the pressure in the release orifice, it is possible to obtain the temperature (T_o) in it using the Antoine equation. Then, given that it is an adiabatic expansion, the calculate of mass vapor fraction will be a function of the vapor enthalpy (ΔH^{vap}), the heat capacity of the liquid (Cp_l), and the difference between the storage temperature and the orifice temperature. Then it is possible to obtain the density of the liquid/vapor mixture.

$$X_{v,o} = \frac{Cp_l(T_s - T_o)}{\Delta H^{vap}} \tag{3}$$

$$\rho_{m,o} = \frac{1}{\frac{X_{v,o}}{\rho_{g,o}} + \frac{1-X_{v,o}}{\rho_{l,o}}} \tag{4}$$

Where $\rho_{g,o}$ and $\rho_{l,o}$ are the gas and liquid densities under orifice conditions (P_o and T_o), whose calculations are based on the ideal gas equation and correlations presented at the literature, respectively.

To obtain the mass flow rate (m_o) at the worst scenario was applied the Equation 5, the base of this equation is the standard relationships for liquid flow through a hole. And to calculate the velocity flow in the hole (v_o) (Eq. 6) was resolved the mass conservation equation.

$$m_o = C_d A_o \sqrt{2\rho_{m,o}(P_s - P_o)} \tag{5}$$

$$v_o = \frac{m_o}{\rho_{m,o} A_o} \tag{6}$$

Now, looking at the second scenario, where the release flow is a superheated liquid in the release orifice, the vapor fraction is zero ($X_{v,o} = 0$). In this scenario, the flow regime is in non-equilibrium, with the pressure in the orifice equal to the ambient pressure ($P_o = P_{amb}$), while the temperature of the fluid in the orifice is equivalent to the storage temperature ($T_o = T_s$). Because of this, the mass flow rate (Eq. 5) and the velocity in the orifice (Eq. 6) are treated as a function of liquid density under orifice conditions and of the difference in the pressure between storage and ambient.

The pseudo source condition used to obtain information in the post-expansion, from which the CFD simulations will be performed, depends on the orifice and environment conditions. Hence, the post-expansion pressure is the ambient pressure, and the jet temperature is equivalent to the saturation temperature of the substance at ambient condition ($T_{sat,amb}$). The velocity (v_e) and the vapor fraction ($X_{v,e}$) in the post-expansion can be obtained by solving the conservation equations of mass, momentum, and energy, and are expressed, respectively, by:

$$T_e = T_{sat,amb} = \frac{B}{A - \log_{10} P_{amb}} - C \tag{7}$$

$$v_e = v_o + \frac{(P_o - P_{amb})}{v_o \rho_{l,o}} \tag{8}$$

$$X_{v,e} = \left(C_p(T_o - T_b) + X_{v,o}\Delta H^{vap,e} + \frac{v_o^2 - v_e^2}{2} \right) \frac{1}{\Delta \mathrm{H}^{\mathrm{vap,e}}} \tag{9}$$

In cases where the post-expansion position in which all liquid droplets are evaporated, $X_{v,e} = 1$, so Eq. 9 is not applied. Then follows the determination of the area formed by the jet in the post-expansion (A_e) and, thus, the expanded diameter (d_e). Subsequently, it is possible to calculate the flow at that position based on the conservation equation.

$$A_e = \frac{\rho_{l,o} A_o v_o}{\rho_{m,e} v_e} \tag{10}$$

$$d_e = \sqrt{\frac{4A_e}{\pi}} \tag{11}$$

$$m_e = \rho_{m,e} v_e A_e \tag{12}$$

The term density of the mixture under post-expansion conditions can be calculated as seen below:

$$\rho_{m,e} = \frac{1}{\frac{X_{v,e}}{\rho_{g,e}} + \frac{1-X_{v,e}}{\rho_{l,e}}} \tag{13}$$

The pseudo-source approach is also used to estimate the conditions at post-expansion for a single-phase gas simulation. The calculation of conditions in this region considers that the liquid fraction is equal to zero. From this, equivalent diameter and mass flow value are determined from Eq. 11 and 12, respectively. The temperature at the pseudo-source corresponds to the saturation temperature of the substance under post-expansion conditions and can be calculated using the Antoine equation.

4 Methodology

The present work was based on the development of CFD simulations for area classification studies. Considered half of the study domain, whose dimensions and boundary conditions are presented in Fig. 1. Propane was the substance defined to compose the release scenario.

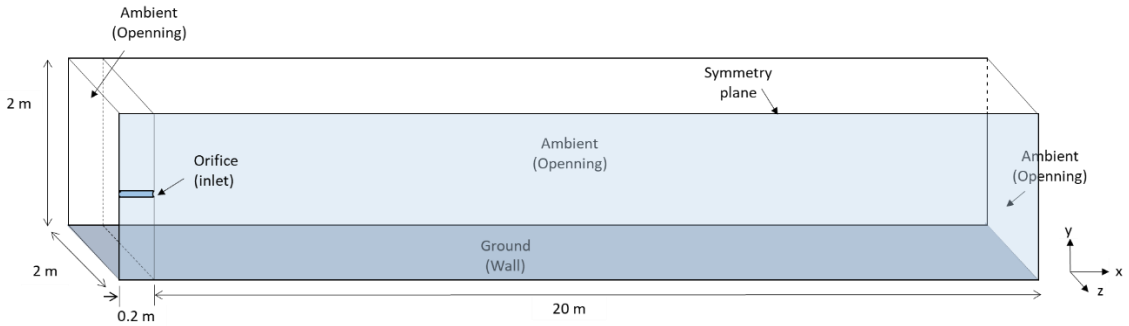

Figure 1. Computational domain and its respective boundary conditions.

The constructed geometry has a cone close to the hole, aiming at a better mesh refinement in this region, and took into account the release hole in post-expansion conditions, where the hole diameter is d_e (Eq. 11). It was adopted a symmetry condition in the plane where the release orifice is, and the orifice is treated as an inlet. The entire environment is taken to be opening, while the floor is a wall condition. The gravitational and ground effects considered provide a more realistic treatment.

A grid independence test was performed varying the mesh refinement in the ambient, near the hole, and on the ground. The Table 1 contains the mesh information and the simulation results of each case. Based on the extent results, it is possible to observe that the refinement performed on the ground (Meshes 3 and 4) results in a longer plume extent for ¼ LEL, which points to a more conservative scenario. Evaluating the extent results for ½ LEL, whose differences were found in the second decimal place, and the volume results at ¼ LEL, so could be seen that mesh 4 best described the case. Mesh 4 expressed the conservatism and coherence of the results, with intermediate result values, without underestimating or overestimating the extent and volume values, and was the choice of mesh for the simulations in this work.

Table 1. Grid independence test (propane, homogeneous equilibrium condition, P_S = 14 bar, d_o = 1.3 mm, T_S = 312.92 K).

Mesh/ simulation Information	**Mesh 1**	**Mesh 2**	**Mesh 3**	**Mesh 4**
Elements	1,060,171	1,611,897	2,129,986	2,340,378
Reached convergence criteria?	Yes	Yes	Yes	Yes
Extent to LFL (m)	1.237	1.243	1.236	1.241
Extent to ½ LFL (m)	2.452	2.484	2.457	2.469
Extent to ¼ LFL (m)	8.103	8.103	8.331	8.317
Volume to LFL (m^3)	0.016	0.016	0.016	0.016
Volume to ½ LFL (m^3)	0.132	0.132	0.132	0.132
Volume to ¼ LFL (m^3)	1.822	1.902	1.829	1.831

4.1 Mathematical modeling

The Eulerian-Lagrangian approach was applied in the multiphase simulations and the Eulerian approach for the gas phase simulations in both single and two-phase simulations. The SST (Shear Stress Transport) turbulence model was used for the continuous phase turbulence calculation, and the particle diameter of the discrete phase was assumed to be constant.

In the first approach, the ambient air/propane mixture in the gas phase is treated as the continuous phase, while the propane droplets as the particulate phase. The continuous phase modeling follows the resolution of the

conservation equations for mass, species, momentum, and energy (Eq. 14 to 17, respectively), and the particulate phase is tracked, generating information about the position, temperature, and mass of each drop. The modeling of liquid particles follows the equation solution of motion and heat and mass transfer, applying the Liquid Evaporation Model. For each particle, the calculations described in ANSYS solver theory guide [7] were performed.

$$\frac{\partial \rho}{\partial t} + \nabla \cdot (\rho \boldsymbol{U}) = 0 \tag{14}$$

$$\frac{\partial (\rho Y_i)}{\partial t} + \nabla \cdot (\rho \boldsymbol{U} Y_i) = \nabla \cdot (\Gamma_{iM} \nabla Y_i) \tag{15}$$

$$\frac{\partial (\rho \boldsymbol{U})}{\partial t} + \nabla \cdot (\rho \boldsymbol{U} \otimes \boldsymbol{U}) = -\nabla p + \nabla \cdot \tau + \rho \mathbf{g} \tag{16}$$

$$\frac{\partial (\rho h)}{\partial t} + \nabla \cdot (\rho \boldsymbol{U} h) = \nabla \cdot (\lambda \nabla T) + \tau : \nabla \boldsymbol{U} \tag{17}$$

4.2 Boundary conditions

The release scenario of the present work comprises the release of propane stored in its liquefied form at 8 bar and 290.65 K, through an orifice of 0.5 mm in diameter. The propane release occurs to the ambient atmosphere at 1atm and 298.15 K. The CFD simulations started from post-expansion, so the release parameters were calculated by the equations contained in topic 3. The post-expansion parameters were input data for CFD Simulations. The homogeneous equilibrium and non-equilibrium scenarios, and the post-expansion region for both the fully evaporated and non-evaporated liquid case, were evaluated and simulated. Therefore, Tab.1 presents the values of the boundary conditions calculated in the post-expansion. Wind speed was neglected in the simulations.

Table 2. Boundary conditions at post-expansion values.

	Case 1 (homogenous equilibrium)	**Case 2** (for $X_{v,e} = 1$ in homogeneous equilibrium)	**Case 3** (non-equilibrium)	**Case 4** (for $X_{v,e} = 1$ in non-equilibrium)
Temperature (K)	231.11	231.11	231.11	231.11
Vapor fraction(wt%)	0.40	1	0.45	1
Velocity ($m.s^{-1}$)	122.02	122.02	52.71	52.71
Particle diameter (μm)	74.62	-	56.81	-
Expanded diameter (mm)	1.5	2.4	4.9	7.4
Total mass flow ($kg.s^{-1}$)	0.0013	0.0013	0.0052	0.0052

5 Results and discussion

The liquid temperature profiles verified in Fig. 2 are based on the trajectory of the particles for cases 1 and 3. It is possible to observe, from the red and blue curves, equilibrium and non-equilibrium conditions respectively, the decrease temperature of the droplets as they advance towards the release jet. This liquid temperature behavior, as described by Barros et al. (2019) [7], is due to the liquid absorbs latent heat from the droplets themselves and from the propane gas released, so that a phase change occurs. It is also verified, in Fig.2, the difference in the droplets range in the different approaches. In case 1 the droplets had a maximum reach of 0.23 m, in case 3 it extended up to 0.69 m, represented by dotted blue. In the latter, the blue dotted pattern represented the greatest range observed for the non-equilibrium condition, where the temperature on this droplet trajectory was constant. The curve completely filled in blue expresses the temperature behavior of most droplets in case 3. As they are in different conditions, due to the greater liquid flow, case 3 presented a greater range of droplets.

In Fig. 3, the propane gas temperature profiles for the four studied cases are evaluated along the central axis of the leak. It is possible to verify in the simulated two-phase cases (cases 1 and 3) an initial temperature increase behavior. It happens due to the adjustment of the two-phase flow to an actual initial condition, which occurs

through the solution of the mass, moment, species, and energy balances that start from the initial estimate of the release parameters in the post-expansion expressed in Tab. 1. Thus, this adjustment leads to the actual post-expansion initial temperature of 253.13K in case 1 and 256.21K in case 3.

Once is reached the post-expansion actual temperature, a temperature drops to a minimum value below the actual temperature and then increase to ambient temperature. This behavior is characteristic of a flash release that develops due to sudden depressurization of the liquefied gas, consistent with is reported in the literature. When looking at cases 2 and 4, the temperature profile shows an increase for ambient temperature, which is consistent with is observed in the literature, as the starting point is post-expansion.

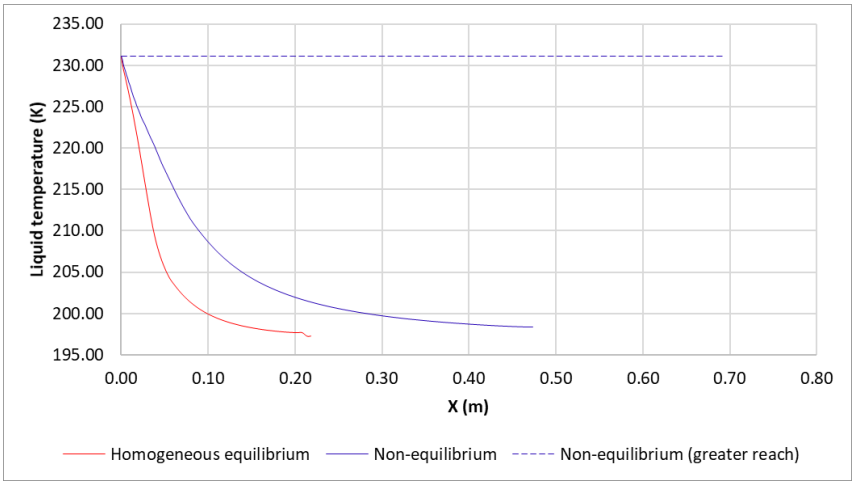

Figure 2. Liquid temperature profile.

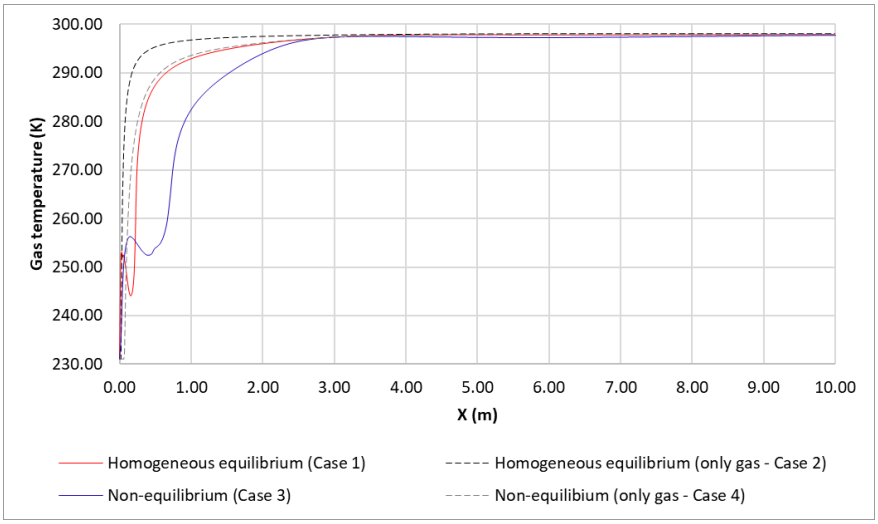

Figure 3. Gas temperature profile.

In Tab. 2, the extent and volume results are evaluated in LFL (2.1% vol. for propane) and at 0.5LFL for the formed gas cloud, as well as the simulation time necessary to reach convergence. Observing the extent and volume results from the non-equilibrium condition, they are higher than the results at equilibrium condition. This occurs due to the higher flow rate, which has a greater amount of liquid and consequently, a larger vapor production than the equilibrium condition.

By analyzing cases 2 and 4 that started from the position where the propane droplets were totally evaporated, it is possible to obtain similar values of extent and volume to those generated by the two-phase simulations. The difference observed between the approaches was 4.42% on average, which represents a satisfactory result regarding the simulation time that a two-phase approach spends in comparison with a single-phase one. The single-

phase approach had a much shorter simulation time than the two-phase approach. In the cases where the condition was equilibrium, the two-phase simulation time was little more than twice the time of the single-phase one. While in the non-equilibrium cases the time was approximately fourteen times the time of the single-phase simulation. Regarding this, for area classification purposes that aim to obtain the extent and volume of the plume data, and having the prior knowledge that there will be no pool formation, the single-phase approach proved to be efficient. Exceptions to the application are given in cases where it desires to observe the behavior of the two-phase region, or in cases where it is not possible to predict the occurrence of pool formation due to the conditions that involve the release.

Table 3. Extent and volume results of the cloud, and simulation time.

	Extent to LFL (m)	Extent to ½ LFL (m)	Volume in LFL (m^3)	Volume in ½ LFL (m^3)	Simulation time
Case 1	0.474	0.937	7.76E-04	6.67E-03	42h 18min
Case 2	0.485	0.957	9.14E-04	7.27E-03	18h 18min
Case 3	1.449	3.677	2.27E-02	2.58E-01	41h 42min
Case 4	1.575	3.510	2.66E-02	2.32E-01	3h 36min

6 Conclusions

The simulations developed in this work were able to reproduce the behavior observed in the literature, being possible to verify the liquid droplets temperature decrease and the range, and the flash phenomenon expected to occur in sudden depressurization of liquefied gas.

In cases of the non-equilibrium conditions, the extent and volume results of the plume were higher than an equilibrium condition. It is consistent with a higher flow rate in the non-equilibrium and elevated fraction of vapor in the release orifice for equilibrium condition. This fact points to the worst leakage scenario in the two-phase jet release study for area classification.

The single-phase approach application to obtain data on the extent and volume of the plume is valid when it is known that there will be no pool and when there is no intention to assess the two-phase region. The single-phase approach efficiency was demonstrated in the similarity of the results for gas cloud extent and volume, and mainly in the considerable reduced simulation time when compared to the two-phase approach.

Acknowledgements. The authors would like to thank LENP (Laboratório de Experimentação Numérica), CNPq, Capes and Petrobras for financial support for this study.

References

[1] C. J. H. Van Den Bosch and R. A. P. M. Weterings, “Methods for the calculation of physical effects (Yellow Book)”. Committee for Prevention of Disasters, The Hague (NL), 3.ed., 2005.
[2] A. W. Cox, F. P. Lees and M. L. C. Ang, “Classification of hazardous locations”. Rugby, IChemE, 1990.
[3] R. Britter, J. Weil, J. Leung and S. Hanna. “Toxic industrial chemical (TIC) source emissions modeling for pressurized liquefied gases”. Atmospheric Environment, pp. 1-25, 2011.
[4] IEC 60079-10-1/Ed2 Explosive atmospheres – Part 10-1: Classification of Areas –Explosive Gas Atmospheres, 2015.
[5] R. K. Calay and A. E. Holdo, “Modelling the dispersion of flashing jets using CFD”. Journal of Hazardous Materials, pp. 1198-1209, 2008.
[6] S. Mannan and F. P. Lees, “Lees loss Prevention in the Process Industries: Hazard Identification, Assessment, and Control”. 3th ed. V. 1, Elservier Butterworth-Heinemann, Amsterdam, 2005.
[7] ANYS CFX – Solver Theory Guide. Version 2020 R2. ANSYS Inc., Canonsburg, USA. 2020.
[8] P. L. Barros, C. A. Nascimento, R. R. Freire, F. J. Queiroz, A. T. P. Neto and J. J. N. Alves, “Numerical simulation of chocked two-phase flow for hazardous area classification”. Ibero-Latin America Congresso n Computational Methods in Engineering – XL CILAMCE, 2019.